Table II: Order of Effectiveness of the Polymers in the Conversion of Six- to Four-Coordinate Species

polymer	NiTMpyP(4)	NiTMpyP(2)
most effective		
$[poly(dAdT)]_2$	all four[a]	mostly four[c]
CT DNA	all four	mostly four[c]
$[poly(dGdC)]_2$	all four[a]	mostly four[c]
poly (U)	all four	mostly four[d]
dextran sulfate	all four[b]	mostly four[d]
phosvitin	mostly four[b]	four ≈ six[d]
heparin	mostly four[b]	all six
poly(D-glutamic acid)	mostly four[b]	all six
less effective		

[a] See Figure 6. [b] See Figure 7. [c] See Figure 9. [d] See Figure 10.

In conclusion, resonance Raman spectroscopy could be very valuable in assessing the binding of such porphyrins to viruses and other well-defined nucleic acids as well as to proteins. Such studies are planned. The special characteristics found for the NiTMpyP(4) interaction with $[poly(dAdT)]_2$ appear to be relatively unique and are not reproduced even with flexible single-stranded nucleic acids. At high R values, such nucleic acids appear to interact with an outside-bound, six-coordinate form of NiTMpyP(4). However, a relatively unperturbed four-coordinate form of NiTMPyP(4) appears to be the most common polymer-bound form, regardless of the nature of the polymer.

Acknowledgment. This work was supported by NIH Grant AI 27196 to L.G.M. and Grant GM 38555 to K.T.Y. We thank the National Institutes of Health for an instrument grant to purchase the CD spectropolarimeter.

Registry No. NiTMpyP(4), 48242-71-3; NiTMpyP(2), 128235-51-8; poly(dU), 35297-30-4; poly(U), 27416-86-0; $[poly(dAdT)]_2$, 26966-61-0; $[poly(dGdC)]_2$, 36786-90-0; Ni, 7440-02-0; NaCl, 7647-14-5; dextran sulfate, 9042-14-2; heparin, 9005-49-6; poly(D-glutamic acid), 25104-13-6; poly(D,L-glutamic acid) SRU, 27030-24-6.

Contribution from the Institute of Chemistry, University of Wrocław, 14 F. Joliot-Curie St., Wrocław 50 383, Poland, and Institute of General Chemistry, I-17, Technical University of Łódź, Łódź 90 924, Poland

Reactions of the Iron(III) Tetraphenylporphyrin π Cation Radical with Triphenylphosphine and the Nitrite Anion. Formation of β-Substituted Iron(III) Porphyrins

Andrzej Małek,[†] Lechosław Latos-Grażyński,*[,†] Tadeusz J. Bartczak,[‡] and Andrzej Żądło[‡]

Received September 26, 1990

The formation of iron(III) β-(triphenylphosphonio)tetraphenylporphyrin (β-PPh_3^+-TPP)Fe^{III} and iron(III) β-nitrotetraphenylporphyrin (β-NO_2-TPP)Fe^{III} in the reaction of iron(III) tetraphenylporphyrin cation radical (TPP$^{\bullet}$)$Fe^{III}(ClO_4)_2$ with triphenylphosphine or nitrite anion has been established through a variety of spectroscopic investigations. The reaction mechanism seems to be analogous to that elucidated for a variety of metalloporphyrin cation radicals or arene cation radicals. The structure of (β-PPh_3^+-TPP)$Fe^{III}Cl_2 \cdot CHCl_3$, $C_{63}H_{43}N_4Cl_5PFe$, has been determined at 173 K by X-ray diffraction: monoclinic space group $I2/a$, $Z = 8$, $a = 27.948$ (3) Å, $b = 11.286$ (3) Å, $c = 33.633$ (5) Å, $\beta = 94.31$ (1)°, least-squares refinement of parameters using 3658 reflections (Mo Kα) yielding $R = 0.091$, $R_w = 0.06$. The structural study of (β-PPh_3^+-TPP)$Fe^{III}Cl_2$ revealed its "zwitterionic" nature. The species belongs to a rather small class of high-spin six-coordinate iron(III) porphyrins and is the first example where two apical positions are occupied by chloride anions. The Fe–Cl distances are Fe–Cl(1) = 2.429(3) Å and Fe–Cl(2) = 2.348 (3) Å. The iron atom is precisely located in the plane of an expanded porphyrin core of a saddlelike conformation with mean Fe–N = 2.055 (7) Å. This value is in the range of Fe–N distances found in other known high-spin ferric porphyrins. This geometry is also preserved in chloroform and has been established for bromide and iodide axial ligands. The proton NMR spectra of high-spin and low-spin iron(III) β-substituted porphyrins have been obtained and analyzed. Functional group assignments have been made with the use of selective deuteration and methyl substitution. The pattern of seven pyrrole resonances reflects the asymmetry that results from β-substitution. This pattern is diagnostic for mono-β-substitution. Because of hindrance of the phenyl group, rotation around the pyrrole carbon–phosphorus bond is restricted.

Introduction

One-electron oxidation of iron(III) porphyrins produces either iron(IV) porphyrins or iron(III) porphyrin cation radicals. Intense interest in these compounds has been stimulated by their involvement in various biological processes[1-3] or in catalytic reactions of metalloporphyrins.[4-6] Their electronic structures and spectroscopic and magnetic properties have been elaborated in detail.[7-14] The magnetic interaction between iron and the radical form of the macrocyclic ligand has been related to the porphyrin core structure.[10] A relationship between the pattern of *meso*-phenyl resonances and the nature of magnetic coupling (ferro- vs antiferromagnetic) has been established.[10,15] Imidazole ligands convert the high-spin iron(III) porphyrin cation-radical complexes to low-spin iron(III) porphyrin cation-radical complexes. Addition of imidazole also induces a reduction of iron(III) porphyrin cation-radical complex to the corresponding low-spin iron(III) porphyrin.[12]

Despite the numerous structural investigations, the reactivity of iron(III) porphyrin cation-radical complexes has received little

[†] University of Wrocław.
[‡] Technical University of Łódź.

(1) (a) Dunford, H. B.; Stillman, J. S. *Coord. Chem. Rev.* **1976**, *19*, 187. (b) Dunford, H. B. *Adv. Inorg. Biochem.* **1982**, *4*, 41.
(2) Hewson, W. D.; Hage, L. P. *The Porphyrins*; Dolphin, D., Ed.; Academic Press: New York, 1979; Vol. 7, pp 295–332.
(3) Dawson, J. *Science* **1988**, *240*, 433.
(4) McMurry, J. T.; Groves, J. T. In *Cytochrome P-450: Structure, Mechanism and Biochemistry*; Ortiz de Montellano, P. R., Ed.; Plenum Press: New York, pp 1–27.
(5) Bruice, T. C. in *Mechanistic Principles of Enzyme Activity*; Liebman, J. F., Greenberg, A., Eds.; VCH Publisher Inc.: New York, 1988; pp 227–277.
(6) Arasasingham, R.; Balch, A. L.; Latos-Grażyński, L. In *The Role of Oxygen in Chemistry and Biochemistry*; Ando, W., Moro-Oka, Y., Eds.; Studies in Organic Chemistry 33; Elsevier: New York, 1988; p 417.
(7) Gans, P.; Marchon, J.; Reed, C. A. *Nouv. J. Chim.* **1981**, *5*, 203.
(8) Buisson, G.; Deronizer, A.; Duée, E.; Gans, P.; Marchon, J. C.; Regnard, J. R. *J. Am. Chem. Soc.* **1982**, *104*, 6793.
(9) Scholz, W. F.; Reed, C. A.; Scheidt, R. W.; Lee, Y. J.; Lang, G. *J. Am. Chem. Soc.* **1982**, *104*, 6791.
(10) Gans, P.; Buisson, G.; Duée, E.; Marchon, J.-C.; Erler, B. S.; Scholz, W. F.; Reed, C. A. *J. Am. Chem. Soc.* **1986**, *108*, 1223.
(11) Phillippi, M. A.; Goff, H. M. *J. Am. Chem. Soc.* **1982**, *104*, 6026.

0020-1669/91/1330-3222$02.50/0

study. Two distinct patterns of reactivity of the iron(III) tetraphenylporphyrin π-cation-radical diperchlorate complex have been established by Marchon et al.[16] Outer-sphere one-electron transfer from bromide, iodide, or 1,8-bis(dimethylamino)naphthalene results in formation of iron(III) porphyrin complexes. However, in the presence of bases with a high oxidation potential (such as pyridine), $[(TPP)Fe^{III}-O-Fe^{III}(TPP^{\bullet})]^{+}$ is formed. The proposed mechanism of reaction involves ferryl intermediates ($Fe^{IV}O$) that are formed by internal electron rearrangement of the iron(III) porphyrin cation-radical complex $[(TPP^{\bullet})FeOH]^{+}$. The conversion of the iron(III) porphyrin cation radical to iron(IV) porphyrin also results from the coordination of methoxide.[17] Iron(III) tetramesitylporphyrin, cation radical $(TMP^{\bullet})Fe^{III}(ClO_4)_2$ was used as a convenient oxidizing agent to generate $(TMP^{\bullet})Fe^{IV}O$ from $(TMP)Fe^{IV}O$.[15]

While reactivity of the iron(III) porphyrinate radical complexes has received little study, there has been a considerable body of work done on porphyrin radical complexes of diamagnetic metal ions.[18-24] Typical reactions with a wide variety of nucleophiles produce metalloporphyrins and β- or meso-substituted metalloporphyrins. The formation of meso-substituted isoporphyrins and bilitrienes was also observed for selected nucleophiles.[22] Factors that govern metalloporphyrin cation-radical substitution can be also applicable to reactivity of iron porphyrins cation radicals. This raises the question whether the similar β-substitution or meso-substitution can occur for these iron complexes. Crossley et al. suggested a contribution of an iron tetraphenylporphyrin cation radical in generation of iron(III) β-nitrotetraphenylporphyrin in the reaction of $(TPP)Fe^{III}Cl$ with NO_2.[25] Two equivalents of hydroperoxide oxidize iron(III) tetrakis(4-methoxyphenyl)-porphyrin to the corresponding isoporphyrin.[26]

Here we describe experiments that demonstrate that the addition of two relatively easily oxidized, nucleophiles (triphenylphosphine and nitrite anion) to iron(III) tetraphenylporphyrin cation radical $(TPP^{\bullet})Fe^{III}(ClO_4)_2$ or iron(III) tetra-*p*-tolylporphyrin cation radical $(TTP^{\bullet})Fe^{III}(ClO_4)_2$ form the respective β-substituted derivatives. The mechanism of β-substitution is also discussed.

In order to facilitate the detection of iron(III) β-substituted tetraphenylporphyrins and to gain a better understanding of their properties in solution, we have undertaken an analysis of the paramagnetically shifted ^1H NMR spectra in selected spin/ligation states.

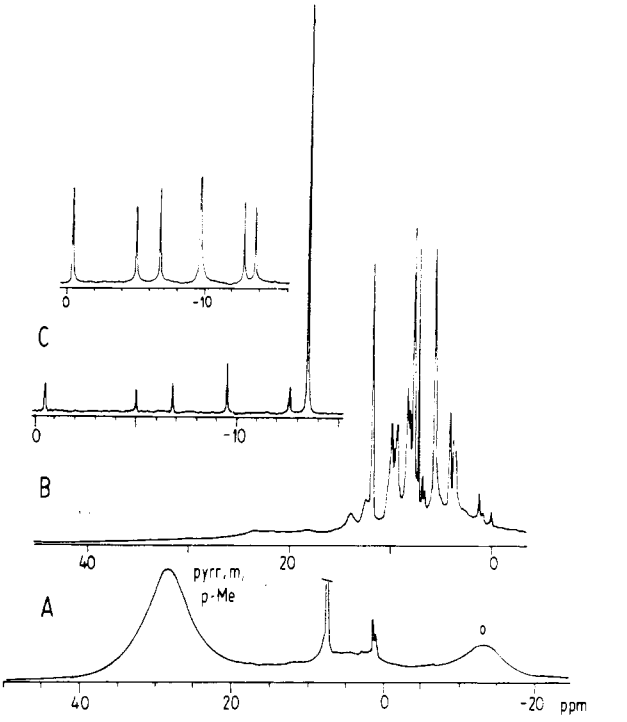

Figure 1. Reaction of iron(III) tetra-*p*-tolylporphyrin π cation radical $(TPP^{\bullet})Fe^{III}(ClO_4)_2$ with triphenylphosphine as followed by ^1H NMR: trace A, a sample of $(TPP^{\bullet})Fe^{III}(ClO_4)_2$ in $CDCl_3$ at 298 K; trace B, the same sample as in trace A after the addition of a 3-fold excess of triphenylphosphine; trace C, the same sample as in trace B after the addition of a 2.5-fold excess of $[(PPh_3)_2N]CN$. Only pyrrole region is shown. The Inset presents the reference spectrum of $(\beta\text{-}PPh_3^{+}\text{-}TPP)Fe^{III}(CN)_2$, which was synthesized by a separate route. Peak labels: pyrr, pyrrole protons; o, ortho protons; m, meta protons; *p*-Me, *p*-methyl protons.

Results and Discussion

Reaction of Iron(III) Tetraphenylporphyrin Cation Radical with Triphenylphosphine and Nitrite Anion. In analogy to previous studies,[18-24] the formation of β-substituted forms, i.e., $(\beta\text{-}PPh_3^{+}\text{-}TPP)Fe^{III}(ClO_4)_2$ (**1**) and $(\beta\text{-}NO_2\text{-}TPP)Fe^{III}(ClO_4)$ (**2**), of a general formula

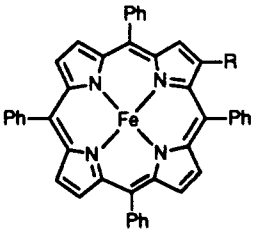

1: R = PPh_3^{+}
2: R = NO_2

can be anticipated in reaction of the iron porphyrin cation radical $(TPP^{\bullet})Fe^{III}(ClO_4)_2$ with two selected nucleophiles: triphenylphosphine (PPh_3) and nitrite. β-Substitution markedly lowers the symmetry of the iron porphyrin from the effective D_{4h} symmetry of parent cation-radical complex. This should be reflected in ^1H NMR spectra, which should show seven pyrrole resonances for each oxidation/ligation/spin state.[27] Addition of triphenylphosphine to a solution of $(TPP^{\bullet})Fe^{III}(ClO_4)_2$ (chloroform, dichloromethane, toluene) resulted in a color change from the green to red. The experiment has been followed by ^1H NMR spectroscopy as illustrated in Figure 1. The typical pattern of $(TPP^{\bullet})Fe^{III}(ClO_4)_2$ has been replaced with a spectrum that is easily assigned to the major reaction product, $(TPP)Fe^{III}(ClO_4)$, which

(12) Goff, H. M.; Phillippi, M. A. *J. Am. Chem. Soc.* **1983**, *105*, 7567.
(13) (a) La Mar, G. N.; deRopp, J. S. *J. Am. Chem. Soc.* **1980**, *102*, 395. (b) La Mar, G. N.; de Ropp, J. S.; Smith, K. M.; Langry, K. C. *J. Biol. Chem.* **1981**, *256*, 237.
(14) Groves, J. T.; Haushalter, R. C.; Nakamura, M.; Nemo, T. E.; Evans, B. J. *J. Am. Chem. Soc.* **1981**, *103*, 2884.
(15) Balch, A. L.; Latos-Grażyński, L.; Renner, M. W. *J. Am. Chem. Soc.* **1985**, *107*, 2983.
(16) (a) Arena, F.; Gans, P.; Marchon, J.-C. *J. Chem. Soc., Chem. Chem.* **1984**, 196. (b) Arena, F.; Gans, P.; Marchon, J.-C. *Nouv. J. Chim.* **1985**, *9*, 505.
(17) Groves, J. T.; Quinn, R.; McMurry, T. J.; Nakamura, M.; Lang, G.; Boso, B. *J. Am. Chem. Soc.* **1985**, *107*, 354.
(18) Evans, B.; Smith, K. M. *Tetrahedron Lett.* **1977**, 3079.
(19) Barnett, G. H.; Evans, B.; Smith, K. M.; Besecke, S.; Fuhrhop, J.-H. *Tetrahedron Lett.* **1976**, 4009.
(20) Evans, B.; Smith, K. M.; Cavaleiro, J. A. *Tetrahedron Lett.* **1976**, 4863.
(21) (a) Johnson, E. C.; Dolphin, D. *J. Tetrahedron Lett.* **1976**, *26*, 2197. (b) Gong, L.-C.; Dolphin, D. *Can. J. Chem.* **1985**, *63*, 401. (c) Dolphin, D.; Halko, D. J.; Johnson, E. C.; Rousseau, In *Porphyrin Chemistry Advances*; Longo, F. R., Ed.; Ann Arbor Science Publisher Inc.: Ann Arbor, MI, 1979; pp 119-141.
(22) (a) Padilla, A. G.; Wu, S. M., Shine, H. J. *J. Chem. Soc., Chem. Commun.* **1976**, 236. (b) Shine, H. J.; Padilla, A. G.; Wu, S. M. *J. Org. Chem.* **1979**, *23*, 4069.
(23) El Kahef, L.; ElMeray, M.; Gross, M.; Giraudeau, *J. Chem. Soc., Chem. Commun.* **1986**, 621.
(24) El Kahef, L.; Gross, M.; Giraudeau *J. Chem. Soc., Chem. Commun.* **1989**, 963.
(25) Catalano, M. M.; Crossley, M. J.; Harding, M. M.; King, L. G. *J. Chem. Soc., Chem. Commun.* **1984**, 1535.
(26) Gold, A.; Ivey, W.; Toney, G. E.; Sangaiah, R. *Inorg. Chem.* **1984**, *23*, 2932.
(27) La Mar, G. N.; Walker, F. A. *The Porphyrins*; Dolphin, D., Ed. Academic Press: New York, 1979; Vol. 4, pp 61-312.

can be identified by the unique position of pyrrole resonance (14 ppm, 298 K) at chloroform (trace B in Figure 1) or in toluene (32.57 ppm, 298 K).[10,28,29] The characteristic non-Curie behavior of this resonance confirms its identification.[28] Spectral properties are consistent with the intermediate spin electronic state of the reaction products. The relatively large line width of intermediate spin iron(III) porphyrins,[28] the location of their resonances in the crowded region of the spectrum in chloroform, and the very low solubility of the anticipated ionic product (β-PPh_3^+–TPP)$Fe^{III}(ClO_4)_2$ in toluene precluded further analysis of the ^1H NMR spectra.

Coordination of strong-field ligands (substituted imidazole, cyanide) converted all of the iron(III) porphyrins in the reaction mixture into low-spin derivatives. Routinely, 2 equiv of substituted imidazole or cyanide were added. The narrow resonances of low-spin iron porphyrins[27] facilitated full identification of the reaction products. At this point, two different low-spin iron(III) porphyrin species are clearly seen (trace B in Figure 1). The pyrrole resonance at −13.42 ppm (298 K) corresponds to $[(TPP)Fe^{III}(CN)_2]^-$. Seven pyrrole resonances of equal intensity in the range 0 to −18 ppm are clearly seen. The spectral pattern is entirely consistent with β-substitution and the formation of (β-PPh_3^+–TPP)Fe^{III}. The identification has been confirmed by an independent synthesis of (β-PPh_3^+–TPP)$Fe^{III}(ClO_4)_2$. (β-PPh_3^+–$TPPH_2$)Cl was obtained by the procedure of Shine et al.[22] followed by iron insertion. The inset in trace C of Figure 1 shows the respective spectra in trace C is particularly significant since this demonstrates that a common product is formed in both routes.

A heterogeneous reaction of the iron porphyrin cation radical with sodium nitrite in chloroform also results in β-substitution. The ^1H NMR spectra of the product are presented and analyzed later on in the paper. A spectroscopically identical product has been synthesized by using the previously described procedure to generate (β-NO_2–TPP)$Fe^{III}Cl$.[25] The nucleophiles used in this study are characterized by relatively weak coordinating properties toward iron(III) porphyrins. This simplified the analysis of the ^1H NMR spectra since additional coordination equilibria could be neglected.[30] An excess of triphenylphosphine has no influence on ^1H NMR spectra of (TPP)$Fe^{III}Cl$ or (TPP)$Fe^{III}(ClO_4)$ in toluene. Thus, the reactions of (TPP$^{\bullet}$)$Fe^{III}(ClO_4)_2$ with triphenylphosphine or nitrite anion are entirely analogous to the well-documented reactions of metalloporphyrin cation radicals or aromatic cation radicals with nucleophiles.[18-25,31]

Triphenylphosphine reduces the iron porphyrin cation radical complex to the corresponding iron(III) porphyrin complex (via eq 1), and (TPP)$Fe^{III}(ClO_4)$ is formed along with the β-substi-

$$(TPP^{\bullet})Fe^{III}(ClO_4)_2 + PPh_3 \rightarrow (TPP)Fe^{III}(ClO_4) + P^{\bullet+}Ph_3 + ClO_4^- \quad (1)$$

tution product. Mechanisms previously proposed for reactions of metalloporphyrin cation radicals or aromatic radicals with nitrite anion or phosphine[22,31] suggest two alternative pathways for β-substitution.

The direct β-substitution with the formation of σ-intermediates has been suggested. In the other mechanism, the reaction of the cation radical with nitrite is preceded by electron exchange, and the product-forming reaction occurs by coupling of the porphyrin cation radical and NO_2 (which also has radical properties).

Scheme I[a]

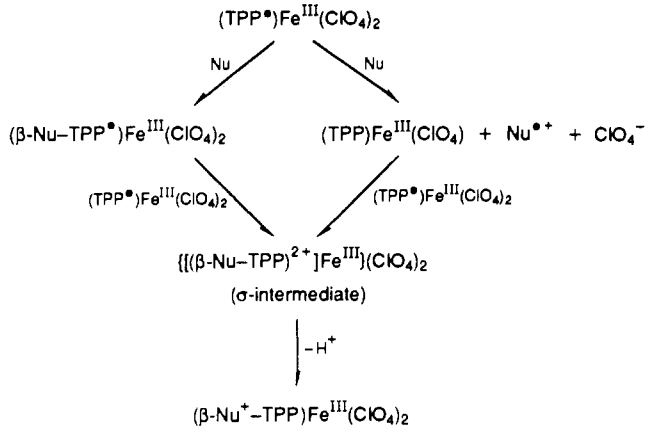

[a] Nu = NO_2^-, PPh_3.

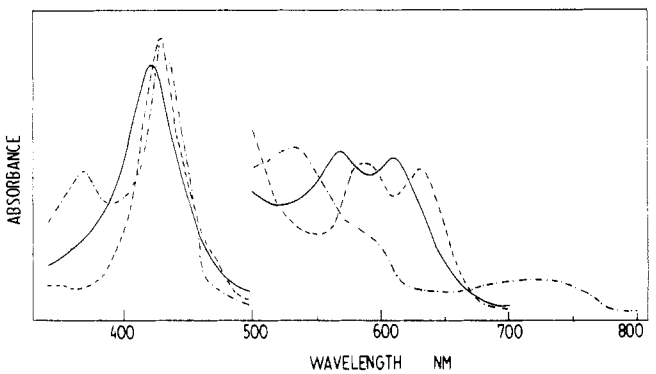

Figure 2. Electronic spectra of chloroform solutions: (—) {[(β-PPh_3^+–TPP)Fe^{III}]$_2$O}$(ClO_4)_2$; (– –) [(β-PPh_3^+–TPP)$Fe^{III}(Im)_2$]Cl_2; (–·–) (β-PPh_3^+–TPP)$Fe^{III}Cl_2$.

Recently Kochi et al. reported the detailed analysis of arene nitration with ion radical pairs ($ArH^{\bullet+}$, $NO_2^{\bullet}$) as reactive intermediates.[31] Crossley et al. suggested that β-substitution with NO_2 is preceded by oxidation of (TPP)$Fe^{III}Cl$ to the corresponding cation radical followed by its reaction with the second molecule of NO_2.[25] Scheme I shows both feasible routes of β-substitution. The overall stoichiometry is shown in eq 2 Integration of the

$$2(TPP^{\bullet})Fe^{III}(ClO_4)_2 + Nu \rightarrow (\beta\text{-}Nu^+\text{–}TPP)Fe^{III}(ClO_4)_2 + (TPP)Fe^{III}(ClO_4) + HClO_4 \quad (2)$$

pyrrole resonances for the case of triphenylphosphine as nucleophile shows a 2.2:1 molar ratio of (TPP)$Fe^{III}(ClO_4)$:(β-PPh_3^+-TPP)$Fe^{III}(ClO_4)_2$ instead of the 1:1 ratio predicted by eq 2. The contribution of the outer-sphere reduction (eq 1) clearly accounts for this observation.

Chemical Properties of Iron(III) β-(Triphenylphosphonio)-tetraphenylporphyrin. Treatment of the iron porphyrin cation-radical complex with triphenylphosphine in dichloromethane on a synthetic scale leads to isolation of a (μ-oxo)diiron complex, {[(β-PPh_3^+–TPP)Fe^{III}]$_2$O}$(ClO_4)_2$, by chromatography. According to the previous spectral analysis the formation of the μ-oxo diiron compounds is preceded by β-substitution to form (β-PPh_3^+–TPP)$Fe^{III}(ClO_4)_2$, which undergoes hydrolysis in course of chromatography with formation of (μ-oxo)diiron species. The spectral properties resemble those of $[(TPP)Fe]_2O$. The electronic spectrum is shown in Figure 2. The infrared spectrum provides strong evidence for the presence of a bent μ-oxo-bridged diiron unit. The band assigned to asymmetric stretching vibration of the Fe^{III}–O–Fe^{III} unit has been observed at 868 cm^{-1}.[32] The Mössbauer spectrum (δ = 0.229 mm/s vs α-Fe, QS = 0.705 mm/s,

(28) (a) Goff, H. M.; Shimomura, E. *J. Am. Chem. Soc.* **1980**, *102*, 31. (b) Goff, H. M. In *Iron Porphyrins*; Lever, A. B. P., Gray, H. B., Eds.; Addison-Wesley Publishing Co.: Reading, MA, 1983, Part 1, p 237.

(29) Reed, C. A.; Mashiko, T.; Bentley, S. P.; Kastner, M. E.; Scheidt, W. R.; Spartalian, K.; Lang, G. *J. Am. Chem. Soc.* **1979**, *101*, 2949.

(30) Preliminary ^1H NMR investigations on the reaction of (TPP•)$Fe^{III}(ClO_4)_2$ with the strongly coordinating base pyridine (pyridine-d_5) established also the nucleophilic pathway contribution to the overall reactivity scheme. The characteristic seven resonances (−7.39, −8.14, −9.61, −10.14, −11.83, and −12.85 ppm vs TMS at 298 K), which flanked the pyrrole resonance of $[(TPP)Fe^{III}(pyridine\text{-}d_5)_2]^+$ have been tentatively assigned to $[(\beta\text{-pyridiniumyl-}d_5\text{-TPP})Fe^{III}(pyridine\text{-}d_5)_2]^{2+}$.

(31) (a) Sankararaman, S.; Haney, A. W.; Kochi, J. K. *J. Am. Chem. Soc.* **1987**, *109*, 5235. (b) Masnovi, J. M.; Sankararaman, S.; Kochi, J. K. *J. Am. Chem. Soc.* **1989**, *111*, 2263.

(32) Saxton, R. J.; Olsen, L. W.; Wilson, L. J. *J. Chem. Soc., Chem. Commun.* **1982**, 984.

Table I. Atomic Coordinates[a] in the Unit Cell and Occupation Parameter (OCP) If Not Equal to 100%

	10^4x	10^4y	10^4z	10^3U_{eq},[c] Å²	OCP, %		10^4x	10^4y	10^4z	10^3U_{eq},[c] Å²	OCP, %
Fe[b]	523 (0)	3199 (1)	3815 (0)	24 (0)		C(28)*	2603 (4)	3707 (10)	4121 (3)	38 (3)	43
Cl(1)	696 (1)	2241 (2)	3195 (1)	36 (1)		C(29)*	3062 (4)	4068 (10)	4263 (3)	32 (3)	43
Cl(2)	316 (1)	4110 (2)	4406 (1)	37 (1)		C(30)*	3118 (4)	4966 (10)	4548 (3)	84 (3)	43
N(21)	71 (2)	1805 (6)	3919 (2)	23 (2)		C(31)*	2715 (4)	5501 (10)	4691 (3)	32 (2)	43
N(22)	1094 (2)	2326 (6)	4108 (2)	26 (2)		C(32)*	2256 (4)	5140 (10)	4549 (3)	46 (3)	43
N(23)	975 (2)	4562 (6)	3694 (2)	27 (2)		C(33)	330 (2)	7050 (5)	3138 (1)	23 (2)	
N(24)	−36 (2)	4048 (6)	3510 (2)	21 (2)		C(34)	390 (2)	8050 (5)	3380 (1)	30 (2)	
C(1)	−412 (2)	1686 (8)	3781 (3)	23 (2)		C(35)	385 (2)	9177 (5)	3209 (1)	36 (2)	
C(2)	−562 (3)	506 (8)	3914 (2)	19 (2)		C(36)	321 (2)	9303 (5)	2796 (1)	35 (2)	
C(3)	−182 (3)	−20 (8)	4116 (3)	22 (2)		C(37)	262 (2)	8303 (5)	2554 (1)	47 (2)	
C(4)	211 (3)	787 (8)	4123 (2)	18 (2)		C(38)	266 (2)	7176 (5)	2725 (1)	36 (2)	
C(5)	676 (3)	519 (7)	4297 (3)	23 (2)		C(39)	−1198 (2)	2429 (6)	3458 (2)	46 (2)	
C(6)	1081 (3)	1234 (8)	4294 (3)	27 (2)		C(40)	−1535 (2)	2895 (6)	3700 (2)	87 (3)	
C(7)	1541 (3)	985 (8)	4499 (3)	40 (2)		C(41)	−2020 (2)	2915 (6)	3567 (2)	157 (3)	
C(8)	1818 (3)	1925 (10)	4426 (4)	66 (2)		C(42)	−2168 (2)	2467 (6)	3191 (2)	216 (3)	
C(9)	1548 (3)	2756 (8)	4177 (3)	45 (2)		C(43)	−1831 (2)	2001 (6)	2949 (2)	189 (3)	
C(10)	1721 (3)	3824 (9)	4029 (4)	61 (2)		C(44)	−1346 (2)	1982 (6)	3082 (2)	86 (3)	
C(11)	1457 (3)	4628 (9)	3794 (3)	52 (2)		P	−1103 (1)	−359 (2)	3851 (1)	23 (1)	
C(12)	1641 (3)	5697 (9)	3631 (3)	50 (2)		C(45)	−1586 (2)	342 (5)	4075 (2)	29 (2)	
C(13)	1273 (3)	6249 (8)	3433 (3)	38 (2)		C(46)	−2065 (2)	104 (5)	3954 (2)	77 (2)	
C(14)	853 (3)	5566 (8)	3477 (3)	27 (2)		C(47)	−2431 (2)	604 (5)	4160 (2)	83 (2)	
C(15)	388 (3)	5856 (8)	3321 (3)	26 (2)		C(48)	−2317 (2)	1342 (5)	4486 (2)	66 (2)	
C(16)	−20 (3)	5126 (8)	3335 (3)	21 (2)		C(49)	−1838 (2)	1579 (5)	4607 (2)	90 (2)	
C(17)	−486 (3)	5488 (8)	3175 (3)	22 (2)		C(50)	−1473 (2)	1080 (5)	4401 (2)	60 (2)	
C(18)	−786 (3)	4571 (8)	3254 (3)	29 (2)		C(51)	−971 (2)	−1706 (4)	4122 (2)	22 (2)	
C(19)	−501 (3)	3662 (8)	3457 (3)	25 (2)		C(52)	−1048 (2)	−1779 (4)	4526 (2)	33 (2)	
C(20)	−677 (3)	2564 (8)	3573 (3)	26 (2)		C(53)	−863 (2)	−2733 (4)	4753 (2)	34 (2)	
C(21)	739 (2)	−666 (5)	4496 (2)	20 (2)		C(54)	−601 (2)	−3613 (4)	4575 (2)	35 (2)	
C(22)	498 (2)	−917 (5)	4834 (2)	34 (2)		C(55)	−525 (2)	−3540 (4)	4170 (2)	34 (2)	
C(23)	506 (2)	−2063 (5)	4990 (2)	46 (2)		C(56)	−710 (2)	−2586 (4)	3944 (2)	34 (2)	
C(24)	754 (2)	−2958 (5)	4807 (2)	55 (2)		C(57)	−1229 (2)	−801 (5)	3344 (2)	34 (2)	
C(25)	996 (2)	−2707 (5)	4469 (2)	51 (2)		C(58)	−883 (2)	−598 (5)	3073 (2)	42 (2)	
C(26)	988 (2)	−1561 (5)	4313 (2)	40 (2)		C(59)	−965 (2)	−972 (5)	2678 (2)	53 (2)	
C(27)	2278 (3)	3932 (9)	4005 (3)	31 (2)	56	C(60)	−1392 (2)	−1549 (5)	2554 (2)	71 (2)	
C(28)	2505 (3)	4130 (9)	4382 (3)	65 (2)	56	C(61)	−1737 (2)	−1751 (5)	2825 (2)	150 (3)	
C(29)	2998 (3)	4338 (9)	4426 (3)	76 (3)	56	C(62)	−1656 (2)	−1377 (5)	3219 (2)	110 (3)	
C(30)	3264 (3)	4347 (9)	4091 (3)	75 (3)	56	C(63)[d]	3349 (3)	4492 (10)	1989 (4)	86 (3)	
C(31)	3037 (3)	4148 (9)	3713 (3)	88 (3)	56	Cl(3)[d]	2953 (1)	3452 (3)	1782 (1)	110 (1)	
C(32)	2544 (3)	3941 (9)	3670 (3)	46 (3)	56	Cl(4)[d]	3313 (1)	5680 (4)	1638 (2)	180 (2)	
C(27)*	2200 (4)	4243 (10)	4264 (3)	22 (2)	43	Cl(5)[d]	3224 (2)	4983 (6)	2428 (2)	251 (2)	

[a] Numbers in parentheses are the estimated standard deviations in the last significant figure. [b] For Fe $x = 0.05227$ (4), $z = 0.38146$ (4), $U_{eq} = 0.0245$ (4) Å². [c] U_{eq} is calculated as $(U_{11}(a^*a)^2 + U_{22}(b^*b)^2 + U_{33}(c^*c)^2 + +2(U_{12}a^*b^*ab(\cos\gamma) + U_{13}a^*c^*ac(\cos\beta) + U_{23}b^*c^*bc(\cos\alpha)))/3$: Willis, B. T. M.; Pryor, A. W. *Thermal Vibrations in Crystallography*; Cambridge University Press: Cambridge, England, 1975; pp 101–102. [d] Chloroform molecule.

$\Gamma_1 = 0.309$ mm/s, and $\Gamma_2 = 0.312$ mm/s, at 298 K) is consistent with the (μ-oxo)diiron(III) structure.[33]

Conductivity measurements show that $\{[((\beta\text{-}PPh_3^+\text{–}TPP)Fe^{III}]_2O\}(ClO_4)_2$ is an electrolyte in dichloromethane solution. In the ^{1}H NMR spectrum (Figure 3), a set of pyrrole resonances at ca. 14 ppm (298 K) identifies $\{[(\beta\text{-}PPh_3^+\text{–}TPP)Fe^{III}]_2O\}(ClO_4)_2$ and reflects the asymmetry imposed by β-substitution. The position of resonances and non-Curie behavior of the isotropic shift with temperature are due to antiferromagnetic interaction that is usual for the μ-oxo diiron systems.[34]

The following reactions of the iron porphyrin moiety could be easily followed by means of electronic and ^{1}H NMR spectroscopy.

$$\{[(\beta\text{-}PPh_3^+\text{–}TPP)Fe^{III}]_2O\}(ClO_4)_2 \xrightarrow{HX} (\beta\text{-}PPh_3^+\text{–}TPP)Fe^{III}X_2 \quad (3)$$

$$(\beta\text{-}PPh_3^+\text{–}TPP)Fe^{III}X_2 \xrightarrow{B} [(\beta\text{-}PPh_3^+\text{–}TPP)Fe^{III}B_2]X_2 \quad (4)$$

$X = Cl^-, Br^-, I^-$; B = R-imidazole, cyanide

Generally the electronic spectra show a red shift of bands relative to spectra of non-β-substituted iron porphyrins (Figure 2).

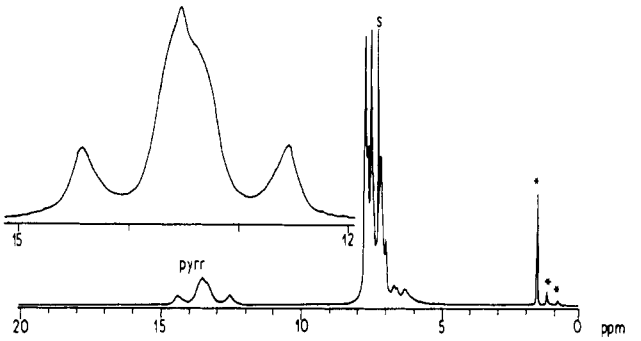

Figure 3. ^{1}H NMR spectrum of $\{[(\beta\text{-}PPh_3^+\text{–}TPP)Fe^{III}]_2O\}(ClO_4)_2$ ($CDCl_3$, 298 K). Peak label: pyrr, pyrrole resonances; s, solvent.

Addition of hydroxide anion to a solution of $\{[(\beta\text{-}PPh_3^+\text{–}TPP)Fe^{III}]_2O\}(ClO_4)_2$ in CD_2Cl_2 (biphasic reaction system CD_2Cl_2/KOD in D_2O) produces new (μ-oxo)diiron species. No attempt has been made to isolate these compounds, but the product of hydrolysis was cleaved with gaseous HBr, dried, and dissolved in $CDCl_3$. Two species, $(TPP)Fe^{III}Br$ (the major product) and $(\beta\text{-}PPh_3^+\text{–}TPP)Fe^{III}Br_2$, were identified by means of ^{1}H NMR spectroscopy. There are precedents for hydrolysis of the phosphonium salt into phosphine oxides with alkyl (aryl) elimination.[35]

(33) Dolphin, D.; Sams, J. R.; Tsin, T. B.; Wong, K. L. *J. Am. Chem. Soc.* **1978**, *100*, 1711.
(34) Chin, D.-H.; Balch, A. L.; La Mar, G. N. *J. Am. Chem. Soc.* **1980**, *102*, 4334. b) Wysłouch, A.; Latos-Grażyński, L.; Grzeszczuk, M.; Drabent, K.; Bartczak, T. *J. Chem. Soc., Chem. Commun.* **1988**, 1377.
(35) Kirby, A. J.; Warren, S. G. *The Organic Chemistry of Phosphines*; Elsvier Publishing Co.: Amsterdam, London, New York, 1967.

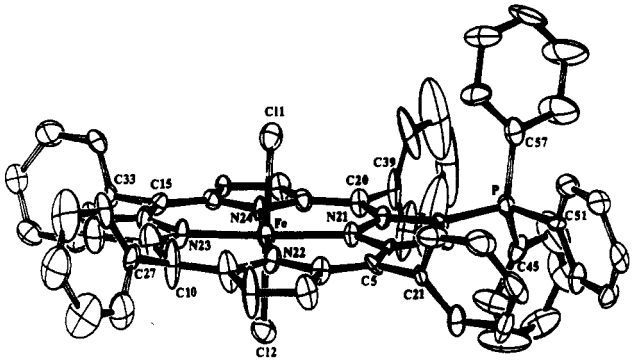

Figure 4. Perspective view of the (β-PPh_3^+–TPP)$Fe^{III}Cl_2$ molecule (50% ellipsoids) with atom numbering.

Table II. Selected Bond Lengths (Å) and Angles (deg) of (β-PPh_3^+–TPP)$Fe^{III}Cl_2$

Bond Lengths			
Fe–Cl(1)	2.430 (3)	Fe–N(22)	2.062 (6)
Fe–Cl(2)	2.349 (3)	Fe–N(23)	2.051 (6)
Fe–N(21)	2.064 (6)	Fe–N(24)	2.042 (6)
Bond Angles			
Cl(1)–Fe–Cl(2)	177.2 (1)	Cl(2)–Fe–N(24)	89.5 (2)
Cl(1)–Fe–N(21)	88.3 (2)	N(21)–Fe–N(22)	90.0 (3)
Cl(1)–Fe–N(22)	90.0 (2)	N(21)–Fe–N(23)	178.2 (3)
Cl(1)–Fe–N(23)	89.9 (2)	N(21)–Fe–N(24)	89.3 (3)
Cl(1)–Fe–N(24)	88.4 (2)	N(22)–Fe–N(23)	89.3 (3)
Cl(2)–Fe–N(21)	89.9 (2)	N(22)–Fe–N(24)	178.4 (3)
Cl(2)–Fe–N(22)	92.0 (2)	N(23)–Fe–N(24)	90.5 (3)
Cl(2)–Fe–N(23)	92.0 (2)		

Thus, this reactivity can be accounted for by an analogous transformation at the phosphonium centers of {[(β-PPh_3^+–TPP)Fe^{III}]$_2$O}$(ClO_4)_2$ as described below:

$$\{[(\beta\text{-}PPh_3^+\text{–}TPP)Fe^{III}]_2O\}(ClO_4)_2 \xrightarrow[-ClO_4^-]{OH^-} \{[(\beta\text{-}PPh_3^+\text{–}TPP)Fe^{III}]\text{–}O\text{–}[(TPP)Fe^{III}]\}ClO_4 + PPh_3O \xrightarrow[-ClO_4^-]{OH^-} [(TPP)Fe^{III}]_2O + PPh_3O \quad (5)$$

Structure of (β-PPh_3^+–TPP)$Fe^{III}Cl_2$. The structure of (β-PPh_3^+–TPP)$Fe^{III}Cl_2$ has been determined by X-ray crystallography. Atomic coordinates are given in Table I. The structure of molecule is shown in Figure 4. Selected distances and angles are given in Table II. Formally, the species has a "zwitterionic" structure. The structural results confirm that the molecule is a six-coordinate one with two axial Cl^- ligands. This is the first example of a six-coordinate, high-spin iron(III) porphyrin complex in which two apical positions are occupied by chloride anions. The iron atom is located precisely in the mean plane of the expanded, saddlelike porphyrin core with a mean Fe–N distance of 2.055 (7) Å. This value is close to the typical values for high-spin, six-coordinated iron(III) porphyrins (iron atom in plane, Fe–N_p > 2.040 Å).[36]

The Fe–Cl(1) = 2.429 (3) Å and Fe–Cl(2) = 2.348 (3) Å bonds are among the longest found in high-spin iron(III) porphyrin complexes (2.192 (12) Å in (TPP)$Fe^{III}Cl$,[37a] 2.218 (6) Å in (ProtoIX)$Fe^{III}Cl$,[37b] 2.229 (5) in chloro-(5,10-dimethyl-5,15-dihydro-2,3,7,8,12,13,17,18-octaethylporphinato-*N′,N″,N‴,N⁗*)iron(III),[37c] 2.242 (1) Å in chloro[3,7-diethyl-1,4,5,8-tetramethyl-2,6-(μ-2,3,5,6-tetramethylbenzene-1,4-bis(tetramethylene))porphinato]iron(III) dichloromethane solvate,[37d] 2.242 (1) Å in (C_2-Cap)$Fe^{III}Cl$,[37e] and 2.259 (2) in chloro((*N*-tosylimido)-tetraphenylporphinato-*N′,N″,N‴,N⁗*)iron(III) hydroxonium chloride methanol solvate[37f] with only one value larger: 2.47 (5) Å in chloro(*meso*-$\alpha,\alpha,\alpha,\alpha$-tetrakis(nicotinamidophenyl)porphyrinato)iron(III)copper(II) perchlorate dihydrate.[37g]

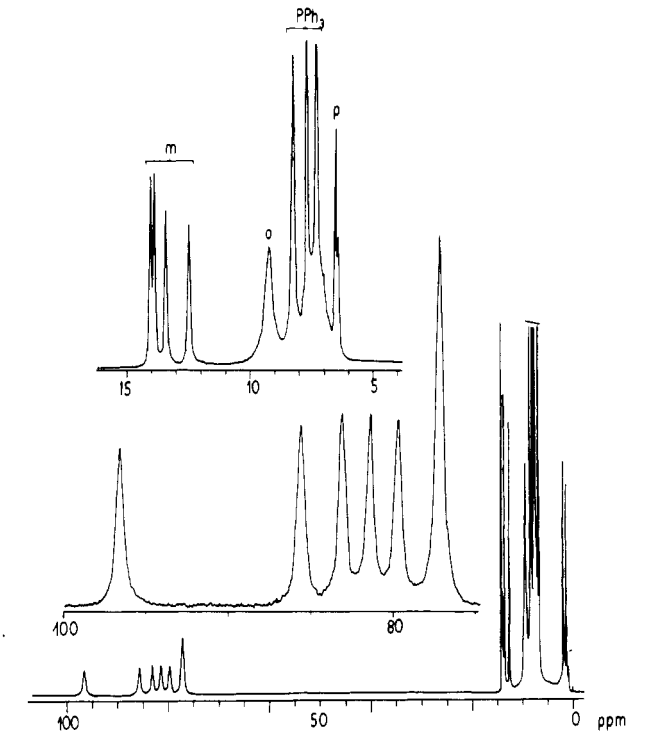

Figure 5. ^1H NMR spectrum of (β-PPh_3^+–TPP)$Fe^{III}Br_2$ ($CDCl_3$, 298 K). Resonance assignments follow those in Table III with o (ortho), m (meta), p (para), and PPh_3 (triphenylphosphine) resonances labeled on the spectrum.

The conformation of the porphyrin macrocycle can be described as a saddlelike. The nearly planar pyrrole rings tilt alternatively up and down the mean plane of the 24-atom porphyrin core. The C(2)–P bond length of 1.799(9) Å is normal. The *phosphonium*–phenyl ring C(45)–C(50) forms an angle of 15.4 (2)° with the *meso*-phenyl ring C(39)–C(45) and the *phosphonium*–phenyl ring C(51)–C(56) forms an angle of 26.6 (2)° with the *meso*-phenyl ring C(21)–C(26). The orientation of these phenyl groups results presumably from short intramolecular contacts. There is a well-defined chloroform molecule present in the structure. The bond lengths and angles within this molecule of solvation are as follows: C(63)–Cl(3) = 1.72 (1), C(63)–Cl(4) = 1.78 (1), and C(63)–Cl(5) = 1.64 (2) Å; Cl(3)–C(63)–Cl(4) = 104.0 (6), Cl(3)–C(63)–Cl(5) = 114.9 (7), and Cl(4)–C(63)–Cl(5) = 109.7 (7)°. There are no intermolecular contacts below 3.5 Å.

Characterization of High-Spin Iron(III) β-Substituted Porphyrins. The ^1H NMR data have been analyzed in the context of the symmetry resulting from the β-substitution (Figure 4) in any spin/ligation state. There are seven distinct pyrrole resonances and four different meso positions. For a five-coordinate species eight ortho, eight meta, and four para protons will be distinguishable because of the essentially perpendicular relation between the meso phenyl plane and the plane of adjacent pyrrole rings and the restricted rotation about the meso carbon-to-phenyl bond. In the case of the rapid rotation, the number of ortho and meta resonances is reduced to four.

Four ortho and four meta resonances are expected for (β-NO_2–TPP)$Fe^{III}B_2$ since the molecule is symmetrical with respect to the porphyrin plane. The configuration of the phosphonium fragment and the freedom of the rotation around the pyrrole-β-

(36) (a) Kastner, M. E.; Scheidt, W. R.; Mashiko, T.; Reed, C. A. *J. Am. Chem. Soc.* **1978**, *100*, 666. (b) Mashiko, T.; Kastner, M. E.; Spartalian, K.; Scheidt, W. R.; Reed, C. A. *J. Am. Chem. Soc.* **1978**, *100*, 6354.

(37) (a) Hoard, J. L.; Cohen, G. H.; Glick, M. D. *J. Am. Chem. Soc.* **1967**, *89*, 1992. (b) Koenig, D. F. *Acta Crystallogr.* **1965**, *18*, 663. (c) Botulinski, A.; Buchler, J. W.; Lee, Y. J.; Scheidt, W. R.; Wicholas, M. *Inorg. Chem.* **1988**, *27*, 927. (d) David, S.; Dolphin, D.; James, B. R.; Paine, J. P., III; Wijesekera, T. P.; Einstein, F. W. B.; Jones, T. *Can. J. Chem.* **1986**, *64*, 208. (e) Sabat, M.; Ibers, J. A. *J. Am. Chem. Soc.* **1982**, *104*, 3715. (f) Mahy, P.; Battioni, P.; Bedi, G.; Mansuy, D.; Fischer, J.; Weiss, R.; Morgenstern-Badarau, I. *Inorg. Chem.* **1988**, *27*, 353. (g) Gunter, M. J.; Mander, L. N.; McLaughlin, G. M.; Murray, K. S.; Berry, K. J.; Clark, P. E.; Buckingham, D. A. *J. Am. Chem. Soc.* **1980**, *102*, 1470.

Table III. Proton NMR Data for High-Spin (β-PPh_3^+-TPP)$Fe^{III}X_2$ Complexes[a]

	Cl^-[b]	Br^-	I^-
pyrrole	95.57	96.56	95.44
	84.22	85.58	85.18
	81.29	83.09	83.08
	80.18	81.36	80.68
	78.68	79.67	78.45
	76.14	77.12	78.87
	76.14	77.12	76.01
ortho[c]		9.22	10.39
			9.26
meta	12.91	14.00	15.00
	12.91	13.84	14.78
	12.43	13.38	13.34
	11.53	12.45	13.36
para[c]		6.51	6.23

[a] In ppm vs TMS at 298 K. [b] Shifts for (β-NO_2TPP)$Fe^{III}Cl$: pyrrole, 102.6 (1 proton), 80.9 (3 protons), 78.9 (3 protons); ortho, 4.75; meta, 13.5, 12.5; para, 6.0, 6.2, 6.3, 6.4. [c] The remaining ortho and para resonances overlap with phenyl resonances of the phosphonium fragment, which are located at 7.2–8.5 ppm.

Table IV. Proton NMR Data for Pyrrole Resonances of (β-PPh_3^+–TPP)$Fe^{III}B_2$ Complexes

Im[a,b]	1-MeIm[a]	2-MeIm[a]	CN^-[a]	CN^-[c]
−9.30	−11.44	−3.63	−0.52	4.17
−11.33	−12.10	−9.07	−5.07	−0.34
−13.73	−14.10	−10.23	−6.82	−1.27
−18.11	−16.40	−12.17	−9.77	−1.97
−19.60	−18.39	−13.43	−9.70	−3.35
−20.08	−20.54	−15.75	−12.89	−4.11
−24.96	−23.09	−17.10	−13.70	−4.93
		Average Shift		
−16.74	−16.56	−11.63	−8.35	−1.68
		Spread of Resonances		
15.65	11.60	13.60	13.2	9.07

[a] In $CDCl_3$. [b] The corresponding line widths (Hz) are 27 (55), 27 (81), 25 (165), 33 (255), 39 (108), 40 (146), and 45 (281). In parentheses are given values established at 213 K. [c] In CD_3OD. All shifts vs TMS at 298 K.

carbon–phosphorus bond determines also the spectrum pattern. In the case of bisligated species, both sides of the porphyrin plane can be distinguished because of the phosphonium group orientation.

Frozen rotation of the phosphonium group and/or meso phenyls will be reflected in the spectrum by eight ortho and eight meta resonance. Fast rotation will simplify the spectra, decreasing the number of these resonances to four. The number of resonances can be considered as a diagnostic feature of number of ligands at available axial positions and/or internal rotation in the (β-PPh_3^+–TPP)Fe^{III}– moiety.

Representative ^1H NMR spectra of high-spin and low-spin (β-PPh_3^+–TPP)Fe^{III} complexes are shown in Figures 3, 5, and 6. Resonance assignments, which are given in Tables III–V, and Figures 3, 5, and 6 have been made on the basis of relative intensities, line widths, site-specific deuteration, and methyl substitution. Direct comparison to iron(III) tetraphenylporphyrin complexes facilitated the assignment.[27] Seven downfield pyrrole resonances have been identified for high-spin (β-PPh_3^+–TPP)Fe^{III} and (β-NO_2–TPP)Fe^{III} species. Six of them are spread near the typical position established for high-spin iron(III) tetraphenylporphyrins. The most characteristic resonance occurs c.a. 15 ppm downfield with respect to the center of the remaining six. It seems logical to assign the one with the largest downfield shift to the unique, β-substituted pyrrole. β-substitution influences σ-delocalization mechanism of spin density at substituted pyrrole and also has a noticeable impact on the remaining three pyrrole rings. The spread of their shifts is relatively larger for (β-PPh_3^+–TPP)FeI_2 then for (β-NO_2–TPP)FeI (9.2 ppm vs 4.5 ppm at 298 K). Chemical shift data for (β-PPh_3^+–TPP)$Fe^{III}X_2$ (X = Cl^-, Br^-, I^-) are recorded in Table III. The line width of the most downfield shifted pyrrole resonance increases in the order $I^- < Br^- < Cl^-$ (128, 200, and 454 Hz, respectively). The trend parallels that seen in high-spin, five-coordinate iron(III) tetraphenylporphyrins and iron(III) *N*-methyltetraphenylporphyrins.[38] The anion dependence of line width is a result of significant, axial-ligand-dependent zero-field splitting of the ground electronic state in these species.

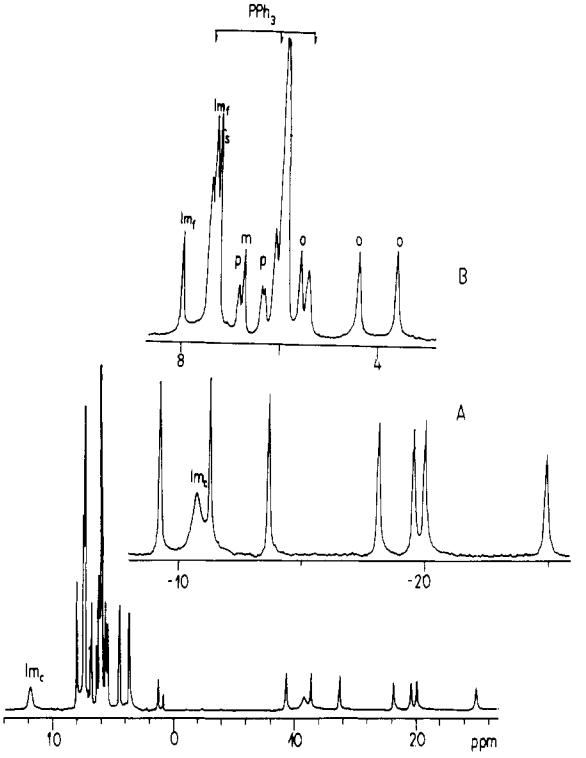

Figure 6. ^1H NMR spectrum [(β-PPh_3^+–TPP)$Fe^{III}(Im)_2$]Br_2 ($CDCl_3$, 298 K). Resonance assignments follow those in Tables IV and VI. Im_c and Im_f indicate resonances of coordinated and free imidazole respectively.

Table V. Proton NMR Data for Pyrrole Resonances of (β-NO_2–TPP)$Fe^{III}B_2$ Complexes

Im[a,c]	1-MeIm[a]	2-MeIm[a]	CN^-[a]	CN^-[b]
−12.31	−12.17	−8.57	−7.64	−2.00
−13.34	−13.27	−9.38	−9.29	−3.93
−16.27	−16.25	−11.23	−11.46	−4.78
−16.27	−16.86	−12.70	−11.73	−5.28
−18.48	−19.03	−14.68	−13.77	−6.50
−19.14	−19.70	−14.76	−14.30	−7.09
−21.17	−21.79	−15.98	−16.15	−7.97
		Average Shift		
−16.71	−17.17	−12.47	−12.05	−5.36
		Spread of Resonances		
8.86	9.61	7.41	8.50	5.97

[a] In $CDCl_3$. [b] In CD_3OD. All shifts vs TMS at 298 K. [c] The line widths (Hz) at 243 K are 33, 34, 47, 52, 46, 50, and 58.

It has been expeditious to examine the data of bromide or iodide forms where the resolution is optimal. Figure 5 shows an expansion of the 20–10 pm region of the (β-PPh_3^+–TPP)$Fe^{III}Br_2$ spectrum. The four, well-separated resonances of comparable line width are assigned to the meta *meso*-phenyl protons of (β-PPh_3^+–TPP)$Fe^{III}Br_2$. A similar pattern has been observed for (β-PPh_3^+–TPP)$Fe^{III}Cl_2$ and (β-PPh_3^+–TPP)$Fe^{III}I_2$. The pattern of meta resonances can be accounted for by coordination of two chloride,

(38) (a) La Mar, G. N.; Eaton, G. R.; Holm, R. H.; Walker, F. A. *J. Am. Chem. Soc.* **1973**, *95*, 63. (b) Behere, D. V.; Birdy, R.; Mitra, S. *Inorg. Chem.* **1982**, *21*, 386. (c) Balch, A. L.; La Mar, G. N.; Latos-Grażyński, L.; Renner, M. *Inorg. Chem.* **1985**, *21*, 2432.

bromide, or iodide ligands at the axial positions of (β-PPh_3^+–TPP)$Fe^{III}X_2$. This geometry has been established for (β-PPh_3^+–TPP)$Fe^{III}Cl_2$ in the solid state. Six-coordinate, high-spin iron(III) porphyrins have been usually generated and stabilized by addition of weak field ligands such as alcohol or dimethyl sulfoxide.[39-42] Also two fluoride ions coordinate to iron(III) porphyrins to form a six-coordinate, high-spin iron(III) porphyrin complex in chloroform.[42]

The ^1H NMR spectra of high-spin six-coordinate iron(III) porphyrins resembled those established for high-spin five-coordinate species. However, some differences in the shifts of pyrrole resonances have been determined ($[(TPP)Fe^{III}F_2]^-$, 85.8 ppm; $[(TPP)Fe^{III}(CH_3OH)_2]^+$, 45 ppm; $[(TPP)Fe^{III}(DMSO)_2]^+$, 64 ppm; all shifts vs TMS at 298 K).[28b,39-42] One can conclude that (β-PPh_3^+–TPP)$Fe^{III}X_2$ fits quite well into a general ^1H NMR scheme characteristic of six-coordinate, high-spin iron(III) tetraphenylporphyrins.

EPR spectra of (β-PPh_3^+–TPP)$Fe^{III}X_2$ are also typical for high-spin iron(III) porphyrin with strong $g = 6$ and weak $g = 2$ signals.[43] The "zwitterionic" structure of (β-PPh_3^+–TPP)$Fe^{III}X_2$ may facilitate an equilibrium as shown below:

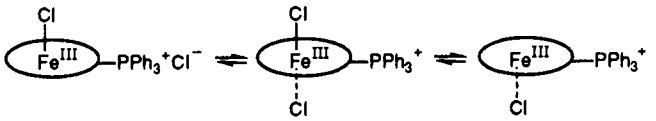

A covalent attachment of the phosphonium group, so close to the iron(III), increases the local concentration and the likelihood of Cl^- coordination without a large excess of external Cl^- ligand, so the solution properties are determined by bisligated species.

Spectral Characterization of Low-Spin Iron(III) β-Substituted Porphyrins. Addition of substituted imidazole or cyanide converts high-spin iron porphyrins into their low-spin counterparts. Comparison of the isotropic shifts gathered in Tables IV and V reveals the fact that dicyano complexes show lower field shifts than the bis(imidazole) complexes. The isotropic shifts of 2-methylimidazole derivatives resemble those of the dicyano analogues in chloroform. The solvent dependence of isotropic shifts of (β-PPh_3^+–TPP)$Fe^{III}(CN)_2$ and $[(\beta\text{-}NO_2TPP)Fe(CN)_2]^-$ is also illustrated in Tables IV and V and can be accounted for by hydrogen bonding in methanol.[44] The difference in isotropic shifts can be attributed to changes in magnetic anisotropy and consequently in dipolar shift rather than to spin delocalization (contact shift). The *meso*-phenyl resonances of paramagnetic metalloporphyrins have been shown to yield characteristic shift patterns that depend on whether the contact or dipolar shift dominates.[45] Alternation of shift direction is characteristic if a π contact shift dominates. The dominant dipolar shift is determined by the symmetry of the magnetic susceptibility tensor and the geometric factor. Usually the shift of phenyl resonances is in one direction and decreases in the order ortho > meta $\simeq$ para. On the basis of phenyl shifts, it is clear that (β-PPh_3^+–TPP)$Fe^{III}(Im)_2$ in chloroform and (β-PPh_3^+–TPP)$Fe^{III}(CN)_2$ in methanol correspond to two extreme cases; i.e., their isotropic shift is determined by dipolar contribution in the first case and contact in the second case. The isotropic shift of the phosphonium moiety shows an upfield bias, which reflects the trend established for *meso*-phenyl resonances. The spread of resonances for a given low-spin β-substituted porphyrin in chloroform appears to be dependent on the axial ligand. Measurable differences have been observed for the respective pairs (β-PPh_3^+–TPP)$Fe^{III}(B)_2$ and (β-NO_2–TPP)$Fe^{III}(B)_2$ (B = substituted imidazole or CN^-). They are determined by the donor/acceptor properties of the β-substituent. The spread of resonances is also solvent dependent as is illustrated by the data of bis(cyano) complexes in chloroform and methanol. It appears to be established by a contact shift. Direct support for a sizable difference in the contact contribution to the different pyrroles results from qualitative consideration of the relative line widths,[27,46] which is produced by the scalar interaction proportional to A^2 (A = hyperfine coupling constant). The spin density pattern of low-spin iron(III) porphyrins with a small spin density at meso positions and a larger spin density at pyrrole positions is consistent with a π delocalization mechanism into the $3e_\pi$ molecular orbitals, which arise from ligand-to-metal π-bonding. β-Substitution splits the $3e_\pi$ orbitals and makes the pyrrole rings unequivalent. An affect of β-substitution was illustrated also in low-spin iron(III) 2,4-substituted natural porphyrin, where four methyl groups were treated as the spectral probes of substitution.[46] An effect of β-substitution is not reflected by any characteristic position of the resonance corresponding to the modified pyrrole of low-spin iron(III) β-substituted tetraphenylporphyrin contrary to the corresponding high spin forms. Likely, the different mechanisms of spin density delocalization (π vs σ), typical for both spin states, produce this difference. The specific coupling between ^{31}P of the phosphonium fragment and the proton located on the same pyrrole (J_{P-H} = 8.4 Hz) has been observed only for (β-PPh_3^+–TPP)-$Fe^{III}(CN)_2$ in chloroform allowing for the unambiguous assignment of the resonance at −5.08 ppm to the pyrrole proton of the modified ring.

The temperature dependences of the chemical shifts for (β-PPh_3^+–TPP)$Fe^{III}(Im)_2$ and (β-NO_2–TPP)$Fe^{III}(Im)_2$ are shown in Figures 7 and 8. The shifts vary linearly with T^{-1}, but the extrapolated lines do not pass through the positions expected for the diamagnetic references. The deviations determined for (β-NO_2–TPP)$Fe^{III}(Im)_2$ seem to be comparable to those established for (TPP)$Fe^{III}(Im)_2$.[47] Further deviations are observed for (β-PPh_3^+–TPP)$Fe^{III}(Im)_2$ (Figure 7), particularly for the resonances of phosphonium moiety. Their shifts do not follow the Curie law; in fact their shifts decrease as the temperature decreases. A selective broadening of phosphonium and pyrrole resonances accompanies the shift changes (Table IV). Both facts can be related to restricted rotation of the phosphonium fragment about β-pyrrole–phosphorus and phosphorus–carbon bonds of the phosphonium group. Because of steric crowding, such rearrangements may involve also some modification of the porphyrin core. It is relatively fast at 298 K but slows down at 223 K, which is demonstrated by typical, for an intermediate rate of rotation, dynamic broadening of resonances. At any frozen configuration each phenyl ring should have different dipolar shift. The observed shift values correspond to the average value as determined by the fast rotation and the populations of the rotamers. The plot of isotropic shifts vs T^{-1} reflects the convolution of two temperature dependent phenomena.

Conclusions

The formation of iron(III) β-substituted porphyrins in the reaction of iron(III) tetraphenylporphyrin cation radical with triphenylphosphine or nitrite anion has been established through a variety of spectroscopic investigations. The reaction mechanism seems to be analogous to that elucidated for metalloporphyrin cation radicals or arene cation radicals. The structural studies of (β-PPh_3^+–TPP)$Fe^{III}Cl_2$ revealed its "zwitterionic" nature. The species belongs to a rather small class of high-spin six-coordinate iron(III) porphyrins and is the very first example where two apical positions are occupied by chloride anions. This geometry is preserved in chloroform and has been established for bromide and

(39) (a) Zobrist, M.; La Mar, G. N. *J. Am. Chem. Soc.* **1978**, *100*, 1944. (b) Budd, D. L.; La Mar, G. N.; Langry, K. C.; Smith, K. M.; Nayyir-Mazhir, R. *J. Am. Chem. Soc.* **1979**, *101*, 6091.
(40) Morishima, I.; Kitagawa, S.; Matsuki, E.; Inubushi, T. *J. Am. Chem. Soc.* **1980**, *102*, 2429.
(41) Behere, D. V.; Birdy, R.; Mitra, S. *Inorg. Chem.* **1984**, *23*, 1979.
(42) Hickman, D. L.; Nanthakuram, A.; Goff, H. M. *J. Am. Chem. Soc.* **1988**, *110*, 6346.
(43) Palmer, G. *The Porphyrins*; Dolphin, D., Ed.; Academic Press: New York, 1979; Vol. 4, pp 313-353.
(44) (a) La Mar, G. N.; Del Gaudio, J.; Frye, J. S. *Biochim. Biophys. Acta* **1977**, *498*, 422. (b) Frye, J. S.; La Mar, G. N. *J. Am. Chem. Soc.* **1975**, *97*, 3651.
(45) Goff, H. M.; La Mar, G. N. *J. Am. Chem. Soc.* **1977**, *99*, 6599.
(46) La Mar, G. N.; Viscio, D. B.; Smith, K. M.; Caughey, W. S.; Smith, M. L. *J. Am. Chem. Soc.* **1978**, *100*, 8085.
(47) La Mar, G. N.; Walker, F. A. *J. Am. Chem. Soc.* **1973**, *95*, 1782.

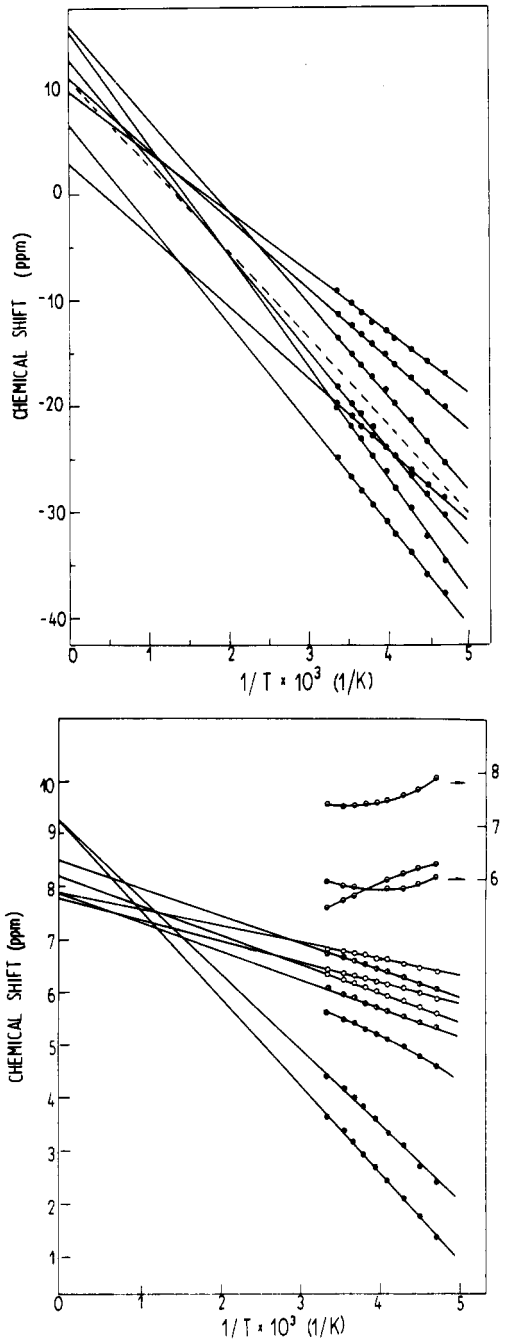

Figure 7. Curie plots of chemical shifts of $[(\beta\text{-}PPh_3^+\text{–}TPP)Fe^{III}(Im)_2]\text{-}Br_2$: (A, top) pyrrole resonances; (B, bottom phenyl resonances. Key: ortho (●); meta (◑); para (○); triphenylphosphine moiety (⊖). The dashed line corresponds to the average pyrrole shift.

iodide axial ligands. It is apparent that the pattern of seven pyrrole resonances in ^1H NMR spectra can be used as a definitive indication of iron(III) β-substituted tetraphenylporphyrins.

In our opinion, the results of this paper emphasize strongly the possibility of β- or meso-substitution in any case where the iron porphyrin cation radicals are involved in the reaction mechanism. Highly oxidized iron porphyrin complexes can generate iron porphyrin cation-radical complexes or protein radicals even if the oxidizing equivalent is initially present as iron(IV) or $Fe^{IV}O$.[48] This suggestion concerns both model iron porphyrins and hemoproteins. The recently established formation of a heme–protein cross-link suggests an involvement of such a mechanism.[49]

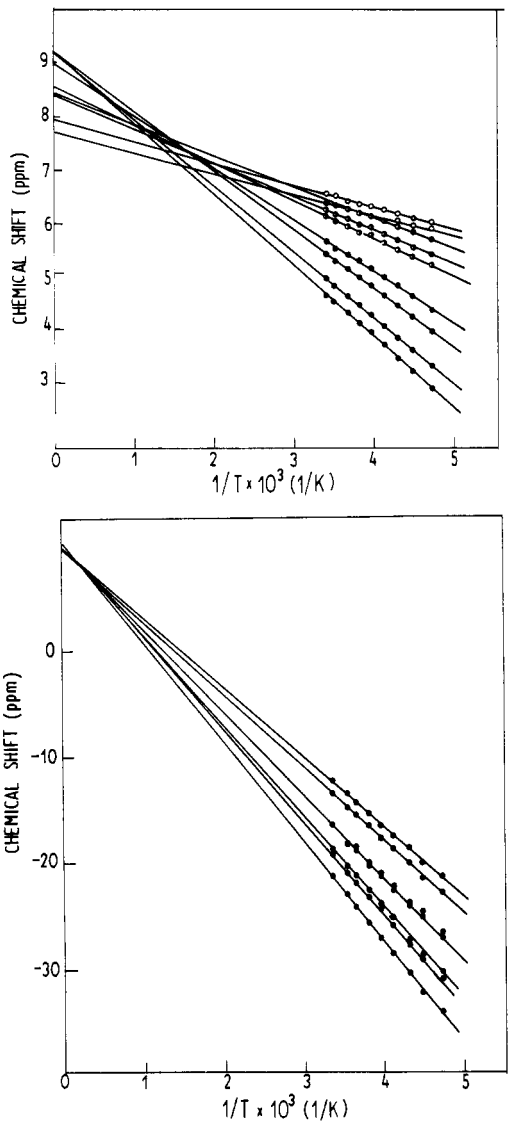

Figure 8. Curie plots of chemical shifts of $[(\beta\text{-}NO_2\text{–}TPP)Fe^{III}(Im)_2]Cl$: (A, top) pyrrole resonances; (B, bottom) phenyl resonances: Key ortho (●); meta (◑); para (○).

Experimental Section

All solvents were purified by standard procedures. Tetraphenylporphyrin ($TPPH_2$), tetra-*p*-tolylporphyrin ($TTPH_2$), and $TPPH_2$-d_{20} were prepared by using routine methods.[50] Benzaldehyde-d_5 was obtained by oxidation of toluene-d_8 with $Ce(SO_4)$.[51] Insertion of iron and zinc into these porphyrins followed established routes. The low-spin iron(III) porphyrins were obtained by addition of the appropriate ligand. The cyanide source in chloroform was bis(triphenylphosphine)nitrogen(1+) cyanide ($[(PPh_3)_2N]CN$). Imidazole and 2-methylimidazole (Aldrich) were recrystallized from benzene. 1-Methylimidazole was used as received from Aldrich. Deuterated solvents were used as received from IBJ (Swierk-Poland).

$(TPP^{\bullet})Fe^{III}(ClO_4)_2$ was synthesized by stirring of $[(TPP)Fe^{III}]_2O$ in dichloromethane with an excess of $Fe^{III}(ClO_4)_3 \cdot 9H_2O$, and recrystallized from dichloromethane/hexane.[10] $(\beta\text{-}PPh_3^+\text{–}TPPH_2)Cl$ was synthesized by the procedure described by Shine et al.[22]

$(\beta\text{-}NO_2TPP)Fe^{III}Cl$ was prepared as described previously.[25]

$\{[(\beta\text{-}PPh_3^+\text{–}TPP)Fe^{III}]_2O\}(ClO_4)_2$. Method I. $(TPP^{\bullet})Fe^{III}(ClO_4)_2$ (880 mg) was dissolved in dichloromethane (300 cm^3). The solution was stirred, and triphenylphosphine (250 mg) in dichloromethane (40 cm^3) was added dropwise. After 30 min, the solution was evaporated to dryness on a rotatory evaporator. The residue was dissolved in dichloromethane and was chromatographed on a column of neutral alumina.

(48) Morehouse, K. M.; Sipe Jr., H. J.; Mason, R. P. *Arch. Biochem. Biophys.* **1989**, *273*, 158.
(49) Catalano, C. E.; Choe, Y. S.; Ortiz de Montellano, P. R. *J. Biol. Chem.* **1989**, *264*, 10534.
(50) Lindsey, J. S.; Schreiman, I. C.; Hsu, H. C.; Kearney, P. C.; Marguerettaz, A. M. *J. Org. Chem.* **1987**, *52*, 827.
(51) Syper, L. *Tetrahedron Lett.* **1966**, 4493.
(52) Bonnett, R.; Dimsdale, M. J. *J. Chem. Soc., Perkin Trans. 1* **1972**, 2540.

Table VI. Crystal Data and Data Collection and Structure Solution Parameters for (β-PPh_3^+–TPP)$Fe^{III}Cl_2$·$CHCl_3$

formula	$C_{63}H_{43}N_4Cl_5PFe$	ρ_{calc}, g cm^{-3}	1.41
fw	1120.15	radiation, Å	0.710 69
cryst syst	monoclinic	μ, cm^{-1}	5.7
space group	*I*2/*a*	transm coeff	0.954–0.989
a, Å	27.948 (3)	scan mode	ω–2θ
b, Å	11.286 (3)	scan angle, deg	1.2
c, Å	33.633 (5)	scan speed, deg mm^{-1}	variable
β, deg	94.31 (1)	max θ, deg	50.0
V, Å^3	10578.5	no. of data measd	9301
T, K	173	no. of data with $F_o > 4\sigma(F_o)$	3658
Z	8	max *h*, *k*, *l*	50, 13, 33
cryst dimens, mm	0.20 × 0.24 × 0.32	*R*	0.091
F(000)	4600	R_w	0.060

Elution with chloroform gave $[(TPP)Fe]_2O$. Elution with 5% v/v of ethanol in chloroform gave two iron porphyrin fractions. The second one was identified as $\{[(\beta\text{-}PPh_3^+\text{–}TPP)Fe^{III}]_2O\}(ClO_4)_2$. Recrystallization from dichloromethane/hexane gave 309 mg of the green powder (37.7% yield).

Anal. Calcd for $C_{124}H_{84}Cl_2Fe_2N_8O_9P_2$: C, 71.78; H, 4.08; N, 5.40. Found: C, 71.15; H, 4.16; N, 5.87. UV–vis, nm (log ϵ): 420 (6.16), 586 (4.11), 632 (4.09).

$\{[(\beta\text{-}PPh_3^+\text{–}TPP)Fe^{III}]_2O\}(ClO_4)_2$. Method II. A modification of the acetate method[52] was applied. $Fe^{II}Cl_2$·H_2O (50 mg), CH_3COOK (1.5 g), and β-PPh_3^+–$TPPH_2Cl$ (50 mg) were added to glacial acetic acid (50 cm^3). The solution was refluxed for 1 h under nitrogen. The iron porphyrin products were extracted into chloroform. This solution was washed with water (to remove acetic acid), evaporated, and chromatographed as described above.

(β-PPh_3^+–TPP)$Fe^{III}Cl_2$. Hydrogen chloride in dichloromethane was added to the solution of $\{[(\beta\text{-}PPh_3^+\text{–}TPP)Fe^{III}]_2O\}(ClO_4)_2$ in dichloromethane (the color changed from green to red), evaporated to dryness, and recrystallized from dichloromethane/hexane. UV–vis ($CHCl_3$), nm (log ϵ): 370 (4.67), 432 (4.96), 528 (3.98), 590 sh (3.69), 706 (3.41), 742 (3.39). Samples of the bromo and iodo derivatives of β-substituted iron(III) porphyrins were obtained from the corresponding (μ-oxo)diiron compounds in an analogous way.

Instrumentation. ^{1}H NMR spectra were recorded on Tesla 567 BS and QE spectrometers operating at 100 and 300 MHz, respectively, operating in the quadrature mode. For a typical spectrum, between 1000 and 5000 transients were accumulated, and the signal to noise ratio was improved by apodization of free-induction decay. ESR spectra were recorded at the X-band on a SE/X Radiopan spectrometer. Absorption spectra were recorded on a Specord M-42 spectrophotometer. Conductivities of solutions were measured with a UK-102/1 Radelkis conductometer. Mössbauer spectra were measured on a 2330 Polon spectrometer with a ^{57}Co(Cr matrix) source.

Crystallographic Study. A dark purple crystal of (β-PPh_3^+–TPP)-$Fe^{III}Cl_2$·$CHCl_3$ was obtained from chloroform/*n*-hexane. Data were collected at low temperature (173 K) on a CAD-4 diffractometer. Crystal data are compiled in Table VI.

Preliminary examination of the crystal on a Weissenberg goniometer established an eight-molecule monoclinic cell, space group *C*2/*c* (or *Cc*). Centering of 25 reflections allowed least-squares calculation of the cell constants (λ = 0.710 69 Å, 173 K): *a* = 42.082 (5) Å, *b* = 11.286 (3) Å, *c* = 27.948 (3) Å, β = 127.16 (1)°. For the unit cell content of eight $[C_{63}H_{43}N_4Cl_5PFe]$ units, the calculated density is 1.41 g/cm^3 (173 K). The density measured by flotation in aqueous solution of potassium iodide is 1.33 (293 K).

Intensity data were measured on the CAD-4 diffractometer using graphite-monochromatized Mo Kα radiation and θ–2θ scanning. The intensities of three control reflections (10,2,3, 8,2,–4, –5,3,1) monitored every hour showed no trend during the data collections. An empirical absorption correction based on intensity profiles for 36 reflections over the full range of setting angles (Ψ) for the diffraction vector was applied to the data. The transmission factors ranged from 0.954 to 0.998. Lorentz and polarization corrections were also applied. Intensity data were reduced and standard deviations calculated.[53] A total of 9524 reflections having (sin θ)/λ < 0.595 Å^{-1} were collected, of which 3658 having $F_o \geq 4\sigma(F_o)$ were retained as observed and used in the solution and refinement of the structure. R_{int} = 0.060; maximum *h* = 50, *k* = 13, and *l* = 33. The structure was solved by direct methods[54] in space group *C*2/*c* and refined by blocked full-matrix, least-squares techniques.[55] At the beginning of the anisotropic refinement high correlation caused by the large value of the monoclinic β angle become apparent. We decided to transform the unit cell to the *I* lattice rather than *C* (by the matrix 001, 010, 101). The respective values are given in Table VI. The *meso*-phenyl and *phosphonium*–phenyl groups were restricted to their idealized geometry (D_{6h}). The phenyl group C(27)–C(32) is disordered among two positions. Refinement of both alternative positions with a variable site occupancy factor (SOF) was carried out. The obtained SOF values were 0.57 and 0.43, respectively. At the end of anisotropic refinement, a difference Fourier synthesis showed the positions of phenyl ring hydrogen atoms. Their positions were idealized (C–H = 0.95 Å, U(H) = 1.5(U_{iso}(C))). All seven phenyl rings were refined in the rigid body model. The final data/parameter ratio was 14.2 for the porphyrin macrocycle. In the final difference Fourier map, the maximum electron density was 0.24 e Å^{-3}, near the Fe atom; the minimum in the map was –0.24 e Å^{-3}. Atomic form factors were as included in SHELX-76.[54] Real and imaginary corrections for anomalous dispersion in the form factor of the iron were applied.[56] In addition to SHELX76, CSU[57] and PARST[58] programs were used. All computations were performed on Amstrad PC1512SD and IBM PS/OS2 Model 80 personal computers.

Acknowledgment. We acknowledge the Polish Academy of Science Grant CPBP 01.12) and the Ministry of National Education (X-ray work, Grant RP.11.10) for financial support.

Supplementary Material Available: Tables of complete bond distances, bond angles, hydrogen atom coordinates, anisotropic thermal parameters, and proton NMR data for low-spin complexes (phenyl resonances) and figures showing a different view of (β-PPh_3^+–TPP)$Fe^{III}Cl_2$·$CHCl_3$, out-of-plane displacements, and a spectroscopic view of the packing in the unit cell (14 pages); a table of observed and calculated structure factors (11 pages). Ordering information is given on any current masthead page.

(53) Calculations for diffractometer operations were performed by using the software supplied with the CAD-4 diffractometer.
(54) Sheldrick, G. M. SHELXS—Program for Crystal Structure Solution. University of Göttingen, Federal Republic of Germany, 1986.
(55) Sheldrick, G. M. SHELX-76. Program for Crystal Structure Determination. University of Cambridge, U.K., 1976. Local MS DOS/PC DOS version adapted by Z. Gałdecki.
(56) Cromer, D. T.; Liberman, D. J.; *J. Chem. Phys.* **1970**, *53*, 1891.
(57) (a) Vickovic, I. CSU, Crystal Structure Utility. University of Zagreb, 1988. (b) Vickovic, I. *J. Appl. Crystallogr.* **1988**, *21*, 987.
(58) Nardelli, M. PARST: A System for Fortran Routines for Calculating Results of Crystal Structure Analysis. *Comput. Chem.* **1983**, *7*, 95.